



RESEARCH MEMORANDUM

SLOTTED-BOUNDARY INTERFERENCE EFFECTS ON WEDGE AIRFOILS

AT LOW SUPERSONIC MACH NUMBERS

By William J. Nelson and Allen R. Vick

Langley Aeronautical Laboratory
Langley Field, Va.

AECER Technical Library
AECER 01

NATIONAL ADVISORY COMMITTEE
FOR AERONAUTICS
WASHINGTON

July 30, 1953
Declassified June 12, 1956



NATIONAL ADVISORY COMMITTEE FOR AERONAUTICS

RESEARCH MEMORANDUM

SLOTTED-BOUNDARY INTERFERENCE EFFECTS ON WEDGE AIRFOILS

AT LOW SUPERSONIC MACH NUMBERS

By William J. Nelson and Allen R. Vick

SUMMARY

Data obtained in an experimental investigation of pressure disturbances caused by the reflection of two-dimensional shock waves from a slotted boundary at Mach numbers between 1.0 and 1.5 are presented herein. Simple-wedge airfoils with apex angles of 4° , 6° , and 10° were used to generate shock waves of different intensity. Static pressures measured at various points along the surface of each airfoil are presented as a function of stream Mach number for several model positions relative to the slotted walls. Comparison of the pressures measured in slotted-tunnel tests with available interference-free data indicated that the 1/5-open slotted boundary used in the present investigation has excessive free area at Mach numbers close to unity where the incident shocks were of the strong family (followed by subsonic flow), but at higher Mach numbers the results indicated insufficient slot area. Although the disturbances associated with reflection of shock waves from the slotted wall were smaller than corresponding free-jet or solid-wall disturbances, it appears from this study that a boundary with variable porosity or variable pressure-drop characteristics or with both will be necessary to eliminate disturbances over wide ranges of Mach number for test models of different geometry.

INTRODUCTION

The feasibility of reducing wind-tunnel interference effects by the use of slotted boundaries was established in reference 1. Those experiments also established that, for models of moderate size, a tunnel with slotted boundaries was free from the choking limitations of closed tunnels. Subsequent investigations at Mach numbers approaching 1.2, references 2 to 5, corroborate the conclusions of reference 1 but give little information regarding the relative strength of incident shock waves and the disturbance associated with their reflection from slotted boundaries. Several investigators have attempted to determine the effect of wall

porosity on the strength of reflected disturbance and, for walls of uniform porosity, the experimental results are consistent with the calculations, references 6 and 7. With the introduction of discrete slots, however, the problem is greatly complicated and the simplified analyses lack experimental verification. A general picture of the mechanics of shock reflection from slotted walls is given in reference 8 where data obtained in tests of several slot configurations at $M = 1.62$ are presented. In the transonic regime the available data lie in the Mach number range below 1.2 and frequently involve tests of three-dimensional models which cause considerable uncertainty in the evaluation of slot performance.

In the present investigation, a series of wedge airfoils has been tested in a slotted tunnel at Mach numbers between 1.0 and 1.5 to determine the effect of shock strength and stream Mach number on the disturbance reflected from the slotted wall. Schlieren photographs and surface pressures have been obtained at Mach numbers close to unity where the bow shock wave was detached from the model and the reflected disturbances are propagated through the subsonic flow field influencing the entire model and also at higher speeds where incident shock waves are reflected in a supersonic field as discrete disturbances. The reflected disturbance is presented as the difference between the measured pressures and the corresponding interference-free pressures and, where practicable, is compared with calculated interferences for both the open jet and the solid wall.

SYMBOLS

H	total pressure
M	Mach number
P_s	free-stream static pressure
P_w	local pressure on wedge surface in slotted tunnel
P'_w	local pressure on wedge surface in free air
P_x	static pressure measured in empty tunnel
c	chord of wedge
h	height of tunnel
t	maximum thickness of wedge
x	distance downstream from vertical plane through apex of wedge

y	vertical distance from wedge to slotted wall
γ	ratio of specific heats (1.4 for air)
C_p	pressure coefficient
\tilde{C}_p	generalized pressure coefficient, $\frac{(\gamma + 1)^{1/3}}{(t/c)^{2/3}} C_p$
ξ_0	transonic similarity parameter, $\frac{M^2 - 1}{[(\gamma + 1)t/c]^{2/3}}$
θ	wedge apex angle

APPARATUS AND METHOD

The photographs of figures 1(a) and 1(b) show the general tunnel arrangement with one side plate partially removed to expose the entrance nozzle blocks and slotted test section; the cylindrical can which enclosed the test section during operation has also been removed. The Mach number in the 4.5- by 2.25-inch test section was varied by controlled removal of air from the can through the use of an auxiliary vacuum system. The center section of the tunnel side walls, in which the models were mounted, was fitted on vertical rails to permit variation in the model position relative to the slotted walls. Eight equally spaced static-pressure taps were mounted in a blank which for tunnel-empty pressure surveys was carried in the 0.4- by 2.5-inch rectangular slot used to support the models in the interference tests. Plate-glass side walls both above and below the wedge support bar permitted schlieren observation of the flow along the slotted walls; the support bar, however, obscures observation for approximately 0.375 inch on either side of the wedge center line.

The top and bottom floors of the tunnel, figure 1(b), were slotted for this investigation. Each floor consisted of seven bars with cross-sectional dimensions of 0.25 and 0.5 inch separated by 0.0625-inch slots giving a free-area ratio of 1:5 for each wall.

Two-inch, steel wedges with apex angles of 4° , 6° , and 10° , figure 1(c), were held in rectangular plastic supports attached to each end and mounted from the side walls at approximately 0° angle of attack. The apex of each wedge was located 6.5 inches downstream from the front of the slots. The sides of the plastic support blocks were made flush

with the inside of the tunnel to avoid pressure disturbances which might interfere with the flow over the wedges. Pressure taps were installed in chordwise rows on each side of the wedge at values of x/c of 0.500, 0.625, and 0.750 with leads extending from the ends of the model.

Pressures were read directly from liquid-filled manometers. The total pressure upstream of the test section and the static pressure in the chamber surrounding the jet were used as references against which the tunnel was calibrated. Schlieren photographs were taken by the use of a single-pass schlieren system with two parabolic mirrors and a light source furnished by a high-voltage discharge through an air-cooled mercury-vapor high-pressure lamp. Continuous visual observation was also possible with this system.

ANALYSIS

At supersonic Mach numbers the problem of jet-boundary interference is largely one of shock-wave reflection at the jet walls. Although other interferences may be of considerable magnitude, only the bow shock reflection will be discussed herein since, being the most upstream disturbance, it will, in general, determine the maximum model size. Much attention has recently been directed toward the use of porous or slotted walls as a means of reducing or eliminating these reflections, and results of several investigations are available which indicate that progress has been made in this direction. These reports, however, have generally been confined to those cases where the flow on both sides of the incident shock wave was supersonic, for example, references 6 to 8. Although the present report contains considerable data taken with supersonic flow along the entire wall, it also includes results obtained at Mach numbers close to unity where detached bow shocks are preceded by supersonic velocities and followed by subsonic flow.

With the flow approaching a wedge at a supersonic Mach number less than that required for attachment, a curved shock wave stands ahead of the leading edge as shown schematically in figure 2. Behind this curved bow shock the Mach number increases monotonically from a subsonic value to the stream Mach number as y increases from 0 to ∞ . The flow deviation through the bow shock increases from 0 at point $y = 0$ to a maximum at $y = a$ and returns to 0 as the Mach number behind the shock approaches the free-stream value. In the same region the static pressure decreases continuously from a maximum at point $y = 0$ to the free-stream pressure at $y = \infty$. The shock profile and flow conditions immediately downstream vary with Mach number and with wedge angle but always with the same general pattern until the Mach number reaches the value at which the bow shock becomes attached and the subsonic flow region is eliminated. In

order to eliminate reflection of a shock wave, it is necessary to preserve the change in flow direction by permitting air from behind the incident disturbance to pass through the slotted boundary. Since the static pressure in the chamber surrounding the tunnel is approximately equal to that in the free stream ahead of the model, the pressure increment available for effecting the transverse flow through the slots is, in the interference-free case, assumed equal to that across the incident shock.

Because of the wide range of flow angles and static pressures encountered at various points behind a detached shock, the required wall porosity is dependent upon the relative size of model and tunnel. For those cases where the boundary flow is entirely supersonic, the pressure increment decreases with the flow deviation and as shown in several reports (e.g., ref. 6) substantial reduction in intensity of the reflected disturbance is possible over a rather wide range of flow conditions using walls of fixed porosity. With subsonic flow downstream of the point of contact between the shock wave and the wall, the same amount of relief would be expected over a much smaller range since, in this region $y < a$, the flow angle and the pressure increment available for effecting the transverse flow through the slots vary in opposite directions.

Although the foregoing discussion has been restricted to phenomena associated with the reflections of bow shocks, it is apparent that elimination of these reflections alone will not permit unlimited increase of model dimensions in a given tunnel. It will, however, eliminate a source of very strong disturbances and will therefore reduce the boundary interference effects.

Interference-free pressure distributions for the wedges tested in this investigation were obtained in the mixed-flow regime from correlation of the data of references 4, 9, and 10 and at the higher Mach numbers from oblique-shock theory using the tables of reference 11. The data of references 4, 9, and 10, correlated on a basis of the transonic similarity parameters \tilde{C}_p and ξ_0 , are presented in figure 3(a). These data were obtained in slotted-tunnel and shock-tube tests and at higher Mach numbers in wind-tunnel tests of models whose dimensions were small in relation to those of the tunnel; the results are considered free from jet-boundary interference effects. The pressure increment between the selected points on the airfoil surface and the free stream, obtained from the generalized coefficients of figure 3(a), are plotted as dotted lines in figure 3(b). These curves, drawn for $x/c = 0.500, 0.625, \text{ and } 0.750$, fair to a common point at the Mach number for which the flow over the wedge becomes supersonic. The calculated curves were arbitrarily faired into the interference-free data of the transonic similarity correlation as shown in figure 3(b) to obtain reference curves against which the slotted-tunnel data will be compared.

RESULTS AND DISCUSSION

Slotted-Tunnel Calibration

The Mach number in this slotted tunnel was determined from the wall static-pressure distributions through the region in which the model was to be tested. These pressures, presented in figure 4 as a ratio p_x/H show little variation along the test region. At Mach numbers of the order of unity, $p_s/H \approx 0.53$, the static pressure in the tunnel was very nearly equal to that in the surrounding chamber. At slightly higher Mach numbers the tunnel pressures were above the chamber pressures but at the maximum speeds tested the relative magnitude of these pressures was reversed. The stream Mach number for the model tests was determined from the measured chamber pressure and its correlation with tunnel-empty data. Previous tests indicate that the relationship between Mach number and chamber pressure ratio is, for the purpose of this investigation, not influenced by the presence of the model.

Shock Patterns

The schlieren photographs of figure 5 show the various bow shock wave configurations encountered at Mach numbers up to 1.36 together with the disturbances reflected from the 1/5-open slotted boundaries. The wedge itself is obscured by the support; however, its approximate position is indicated. At Mach numbers of 1.04 and 1.07 the bow shocks are nearly vertical starting well ahead of the 4° wedge. It is apparent from the slope of these shocks that the flow downstream of the shock wave is subsonic; line reflection of these waves is therefore impossible. At $M = 1.13$ the slope of the bow shock increases with increasing distance from the body; this characteristic, which cannot occur in free air, is clearly associated with excessive flow resistance of the slotted wall. At $M = 1.15$ the asymmetrical shock pattern indicates that the wedge was not perfectly aligned to the stream or that the Mach number in the upper and lower passages was not identical. Again, the slope of the shock wave increases with distance from the airfoil, becoming normal to the stream at the slotted boundary; in the upper passage a Mach reflection indicates that the flow behind the bow shock, although supersonic, was at a Mach number too small to support the turning required at the wall. In the lower passage it appears that the Mach number was subsonic behind the bow shock since subsequent shocks do not appear in the flow. At $M = 1.19$, the incident shock and its Mach reflection are nearly identical in both passages; however, in the upper passage a secondary reflection is visible as the reflected shock is itself reflected from the wedge. In the final photograph of this series, the stream Mach number has been increased to 1.36 and the incident shock is reflected as a shock wave with supersonic flow throughout the field.

Similar pictures were obtained with the 6° wedge mounted off the tunnel axis to permit broader coverage of the reflected disturbances at high Mach numbers, figure 5(b). In the off-center location it is probable that with detached shocks the wedge is, in effect, at a small angle of attack because of the relatively greater flow resistance in the lower passage. With attached shocks, the flow in one passage is not influenced by that in the other and when the reflected disturbances occur as oblique shocks, no disturbance due to the asymmetry would be expected. Again, as in the tests with the 4° wedge, boundary interference effects of varying intensity were encountered at all supersonic Mach numbers. Comparison of these wave patterns for the 4° and 6° wedges shows similar variations with Mach number; however, a given type of reflection occurred at a higher Mach number with the wedge of larger apex angle. Since, at a constant Mach number, the slope of both incident and reflected waves increases with apex angle, interference effects will extend farther forward on the 6° wedge; the length of the model which may be tested in a given tunnel therefore decreases as the wedge angle increases.

In the triangular region between the incident and reflected shock waves the slotted boundary exerts no influence on the flow. Since reflected shocks regardless of their strength lie ahead of the Mach lines, whereas reflected expansions are entirely behind the Mach lines, it is apparent that for interference-free flow the restrictions on model length imposed by reflected shock waves is more severe than the corresponding limitations imposed by reflected expansion. Because of the steepness of the lines along which both types of disturbance are transmitted at transonic Mach numbers, it is frequently impractical to reduce the model length to the region ahead of the reflected disturbance. It is for these conditions and those where subsonic Mach numbers occur along the boundary behind the incident shock that amelioration of the reflected disturbances is imperative.

Surface Pressure Variation With Mach Number

The static-pressure increment $p_w - p_s$ between the free stream and the surface of the test body is expressed in terms of the stream stagnation pressure H and plotted as a function of Mach number in figure 6. The corresponding interference-free curves from figure 3(b), are shown as dotted lines on each diagram to facilitate comparison and interpretation of boundary interferences. In the upper left diagram of figure 6(a) the separation of the two curves for the 4° wedge, $x/c = 0.500$, shows large interference effects which above and below $M = 1.27$ are of opposite sign. In the low Mach number range, it is not surprising that the measured pressures are very close to the pressure in the chamber surrounding the test section since the flow over the model is subsonic and the jet boundary is separated from the model by only $3/8$ of the model chord. Data in this Mach number range are of qualitative interest only with the

model in the off-axis positions since the unequal passages on either side of the model probably result in considerable asymmetry of flow at the leading edge. This restriction, however, does not apply at higher Mach numbers where the bow shock is attached to the leading edge of the test airfoil. At Mach numbers greater than 1.27 the bow shock, reflected from the slotted wall, results in excessive pressure on the model. The rapid decrease in pressure at $M \approx 1.35$ signals the passing of the reflected bow shock across the measuring orifice. At other orifices farther back on the model, the wall interference effects at low Mach numbers were substantially the same as those at $x/c = 0.500$, since the entire flow field along the model is subsonic and boundary pressures are transmitted more or less uniformly over the wedge. For a constant model-boundary separation, the Mach number at which the reflected shock passes the various orifices increases as their distance from the leading edge of the model increases. The decrease in pressure associated with the reflected disturbance passing the more rearward orifices results from a change in deviation across the reflected shock or a decrease at higher Mach numbers in pressure rise across shocks of a given deviation or from both. Doubling the distance between the model and the wall did not sharply alter the shape of the experimental curves; however, it did effect a minor reduction in separation of the data from slotted tunnel and interference-free tests. With the wedge mounted on the tunnel axis the two sides are equidistant from the identical walls; the pressures at corresponding points on the upper and lower surfaces are therefore plotted together on the center row of diagrams, figure 6(a). In the low Mach number range, agreement of these data at the forward orifices indicates that in this position the model was well-aligned to the flow. Differences in pressures at $x/c = 0.750$ indicate lack of uniformity in either the stream itself or in the interference effects; the latter appears more probable since in the tunnel empty the pressures were very uniform, figure 4. At the forward orifices, absence of the characteristic pressure jump associated with movement of the reflected shock across the orifice results from the fact that all bow shocks followed by supersonic flow are reflected downstream of the two forward orifices; at $x/c = 0.750$ the pressure-disturbance characteristic of the line reflection of the bow shock reappears. At greater distances from the walls, $y/c = 1.500$ and 1.875 , the pressure patterns at all orifices were similar to those on the center line.

The 6° wedge was tested in one off-center location only, giving distances of 0.75 and 1.50 chords from the lower and upper surfaces, respectively; these data are presented in figure 6(b). These experimental curves for the 6° wedge are similar to those obtained on the 4° wedge mounted much closer to the tunnel wall. All these curves for the 6° wedge show the abrupt change in surface pressure which characterizes the passage of reflected shock over the measuring orifice. The fact that line reflection of the bow shock occurring on the 6° wedge did not occur at corresponding points on the 4° model results from the increased slope

of the attached bow shock which reduces the longitudinal distance between the apex of the wedge and the point at which the reflected shock returns to the model. In the lower Mach number range where subsonic flow occurs downstream of detached shocks, differences between the experimental slotted-tunnel and interference-free curves increase with wedge angle.

The trends toward increased error in the Mach number range over which the bow shock is detached are continued as the wedge angle is increased to 10° , figure 6(c). With this increase in apex angle the Mach number at which the reflected shock passes a given orifice is further increased. For the top row of diagrams, $y/c = 0.375$, the reflected bow shock fails to pass the orifices within the Mach number range of these tests.

Correlation of the surface pressures with the schlieren photographs of figure 5 shows for the 4° wedge symmetrical wave patterns with detached shocks at $M = 1.04$ and 1.07 and at $M = 1.13$ an attached oblique shock becoming normal at the wall; at these Mach numbers identical pressures were recorded on upper and lower surfaces at $x/c = 0.500$. At $M = 1.15$ and 1.19 the nonsimilar Mach reflections of attached shock which appear in upper and lower passages result in different pressures on the upper and lower surfaces; these differences decrease toward the back of the wedge. At $M = 1.36$ the attached bow shocks are again symmetrically reflected from the upper and lower walls but, in returning to the tunnel center line behind the model, have little effect on the pressure distribution.

Boundary Interference Variation With Mach Number

In figure 7, the difference between slotted tunnel and interference-free pressure measurements is plotted as a function of Mach number for the three wedges investigated. Presented in this manner the interference introduced by model proximity to the slotted boundary may be read directly. At $M = 1.0$ the measured pressure was invariably lower than the corresponding interference-free value; this error increased with Mach number reaching a maximum at values of M slightly less than those corresponding to attachment of the bow shock. With further increases in Mach number, the measured pressure increased rapidly and the error, changing sign, increased until the reflected shock passed the measuring orifice at which point the error decreased abruptly.

In order to facilitate evaluation of this slotted boundary, curves for an open jet and a closed tunnel of the same size relative to the model have been calculated and are shown in figure 7 for those cases where an attached bow shock is reflected ahead of the measuring orifice. It will be noted that the lower end of the Mach number range for which these curves are drawn is different for the open and closed test sections. This situation occurs because the calculations consider only supersonic

reflection; hence a much higher value of M is necessary in the closed tunnel where a shock is reflected as a shock of equal deviation than in the open jet where shocks are reflected as expansions.

Although elimination of boundary interferences is desirable, it appears unlikely that such will be realized over a very broad range of Mach numbers and incident disturbances as discussed earlier in this report. The selection of a porous boundary must therefore be based upon a compromise. For the type of models tested in this investigation and the Mach number range over which these tests were conducted (from $M = 1.0$ to $M = 1.5$), the 1/5-open slotted wall appears to be a fair compromise since the interference effects caused by excessive free area at low Mach numbers are approximately equal to those caused by insufficient free area at higher Mach numbers. Increasing the free area of the slots would undoubtedly increase the errors at low supersonic speeds whereas a reduction in slot area would increase errors at higher speeds. It is probable that a smaller opening would be desirable if the maximum Mach number of the tunnel were reduced substantially.

Increasing the distance between the model and the tunnel wall resulted in substantial reductions in interference effects; however, in these tests no case of interference-free flow was observed simultaneously at all points on the airfoil. Comparison of these curves with those obtained in tests of wedges with greater apex angles shows at $x/c = 0.750$, a small increase in maximum interference effects with the larger angle and an increase in the Mach number at which the maximum error occurs. At $y/c = 1.500$ the interference effects on the 6° wedge were greater than on either the 4° or 10° models. Although the slotted boundary used in this investigation did not prove free from interference effects, the data presented indicate that the magnitude of these effects is generally less than those encountered in jets of comparable size whose boundaries are not slotted. Choking limitations, which in a closed jet would have precluded operation over a large part of the Mach number range investigated, have been removed by the introduction of longitudinal slots through the test section.

CONCLUSIONS

From the results of this preliminary investigation of nonlifting wedges in a two-dimensional wind tunnel with slotted walls, the following conclusions are made:

1. At supersonic Mach numbers close to unity where bow shocks are followed by subsonic flow, the wall interference effects experienced in a tunnel with 1/5-open slotted walls are of the same sign as those experienced in an open jet; their magnitude, which in the presence of slotted

walls increased only slightly with wedge angle, is significantly smaller than would be experienced in an open jet.

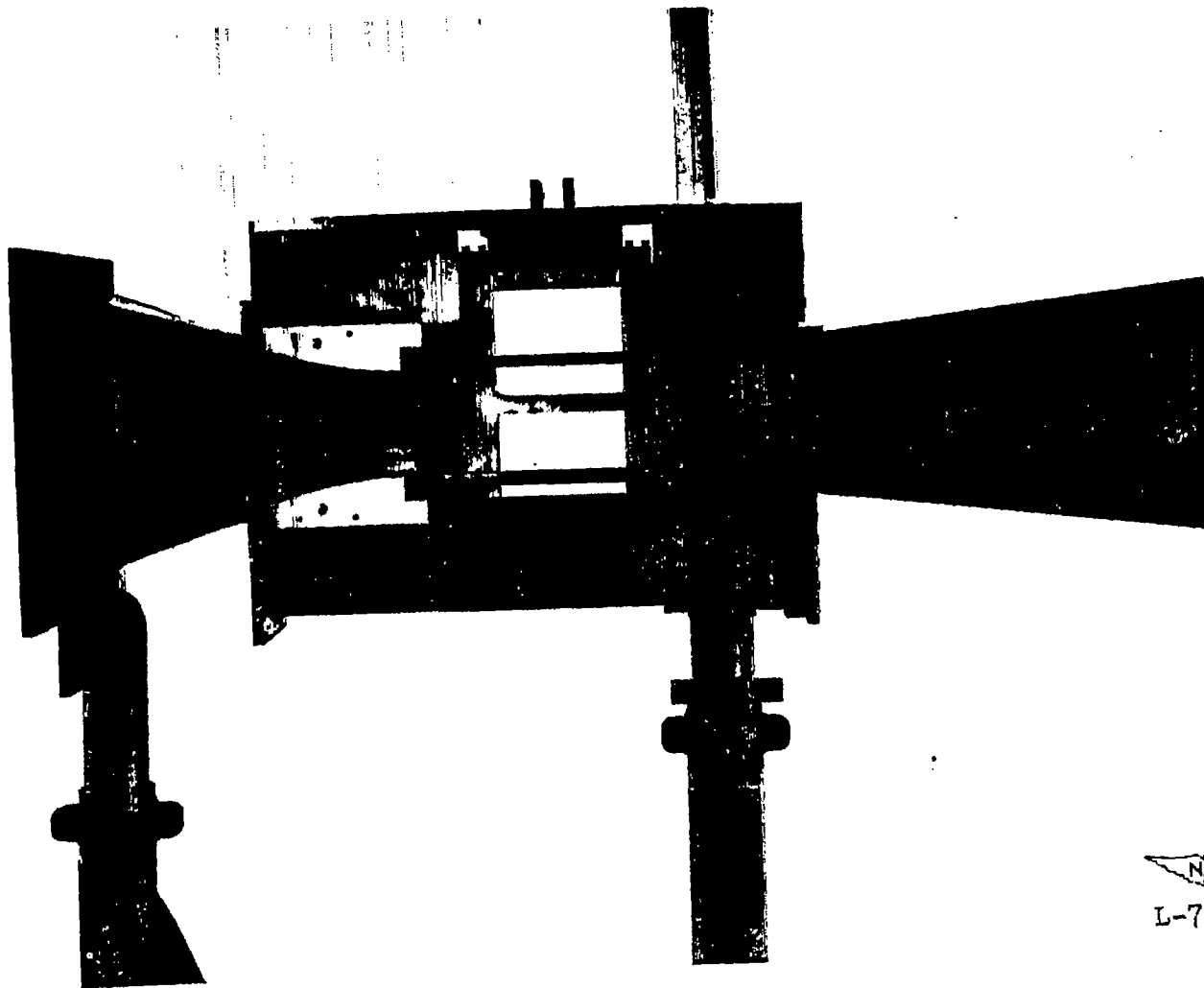
2. Oblique, attached shock waves are reflected from 1/5-open slotted walls as shock waves; however, their strength is less than that of waves reflected from a solid boundary.

3. These results and the accompanying analysis indicate that, although substantial amelioration of reflected shock disturbance can be realized over a wide Mach number range in a 1/5-open slotted tunnel, complete freedom from jet-boundary interference throughout a wide range of Mach numbers will require walls with variable porosity or variable pressure-loss characteristics or with both.

Langley Aeronautical Laboratory,
National Advisory Committee for Aeronautics,
Langley Field, Va., May 29, 1953.

REFERENCES

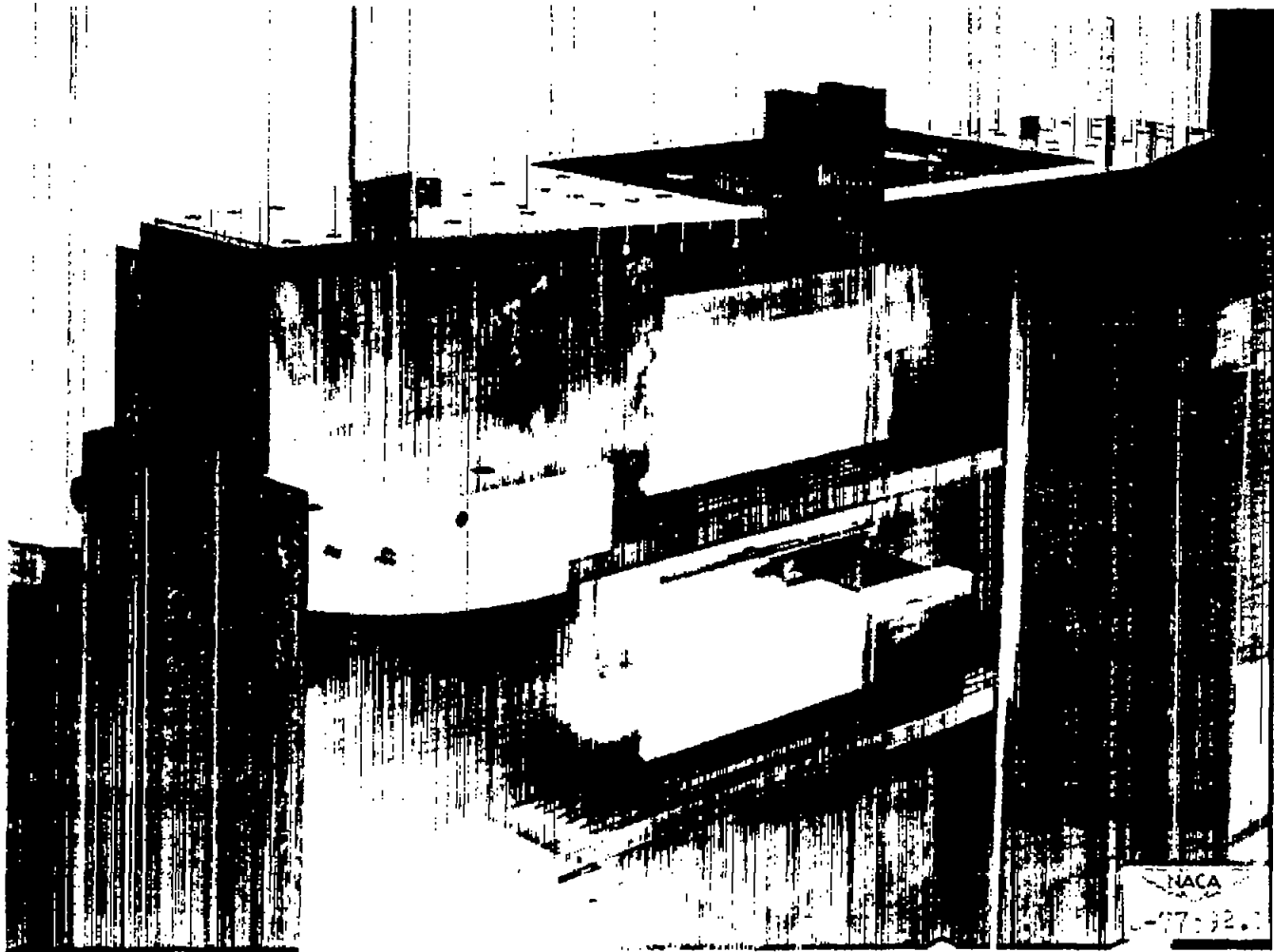
1. Wright, Ray H., and Ward, Vernon G.: NACA Transonic Wind-Tunnel Test Sections. NACA RM L8J06, 1948.
2. Ward, Vernon G., Whitcomb, Charles F., and Pearson, Merwin D.: An NACA Transonic Test Section With Tapered Slots Tested at Mach Numbers to 1.26. NACA RM L50B14, 1950.
3. Hallissy, Joseph M., Jr.: Pressure Measurements on a Body of Revolution in the Langley 16-Foot Transonic Tunnel and a Comparison With Free-Fall Data. NACA RM L51L07a, 1952.
4. Nelson, William J., and Bloetscher, Frederick: An Experimental Investigation of the Zero-Lift Pressure Distribution Over a Wedge Airfoil in Closed, Slotted, and Open-Throat Tunnels. NACA RM L52C18, 1952.
5. Goethert, Bernhard H.: Investigations on Transonic Test Sections at the Wind Tunnel Branch, AMC-Wright Field. Air Materiel Command, Wright Field, Sept. 25, 1950.
6. Nelson, William J., and Bloetscher, Frederick: Preliminary Investigation of Porous Walls As a Means of Reducing Tunnel Boundary Effects at Low-Supersonic Mach Numbers. NACA RM L50D27, 1950.
7. Davis, Don D., and Wood, George P.: Preliminary Investigation of Reflections of Oblique Waves From a Porous Wall. NACA RM L50G19a, 1950.
8. Wood, George P.: Reflection of Shock Waves From Slotted Walls at Mach Number 1.62. NACA RM L52E27, 1952.
9. Griffith, Wayland: Shock-Tube Studies of Transonic Flow Over Wedge Profiles. Jour. Aero. Sci., vol. 19, no. 4, Apr. 1952, pp. 249-257, 264.
10. Liepmann, H. W., and Bryson, A. E., Jr.: Transonic Flow Past Wedge Sections. Jour. Aero. Sci., vol. 17, no. 12, Dec. 1950. pp. 745-755.
11. Neice, Marie M.: Tables and Charts of Flow Parameters Across Oblique Shocks. NACA TN 1673, 1948.



NACA
L-77593

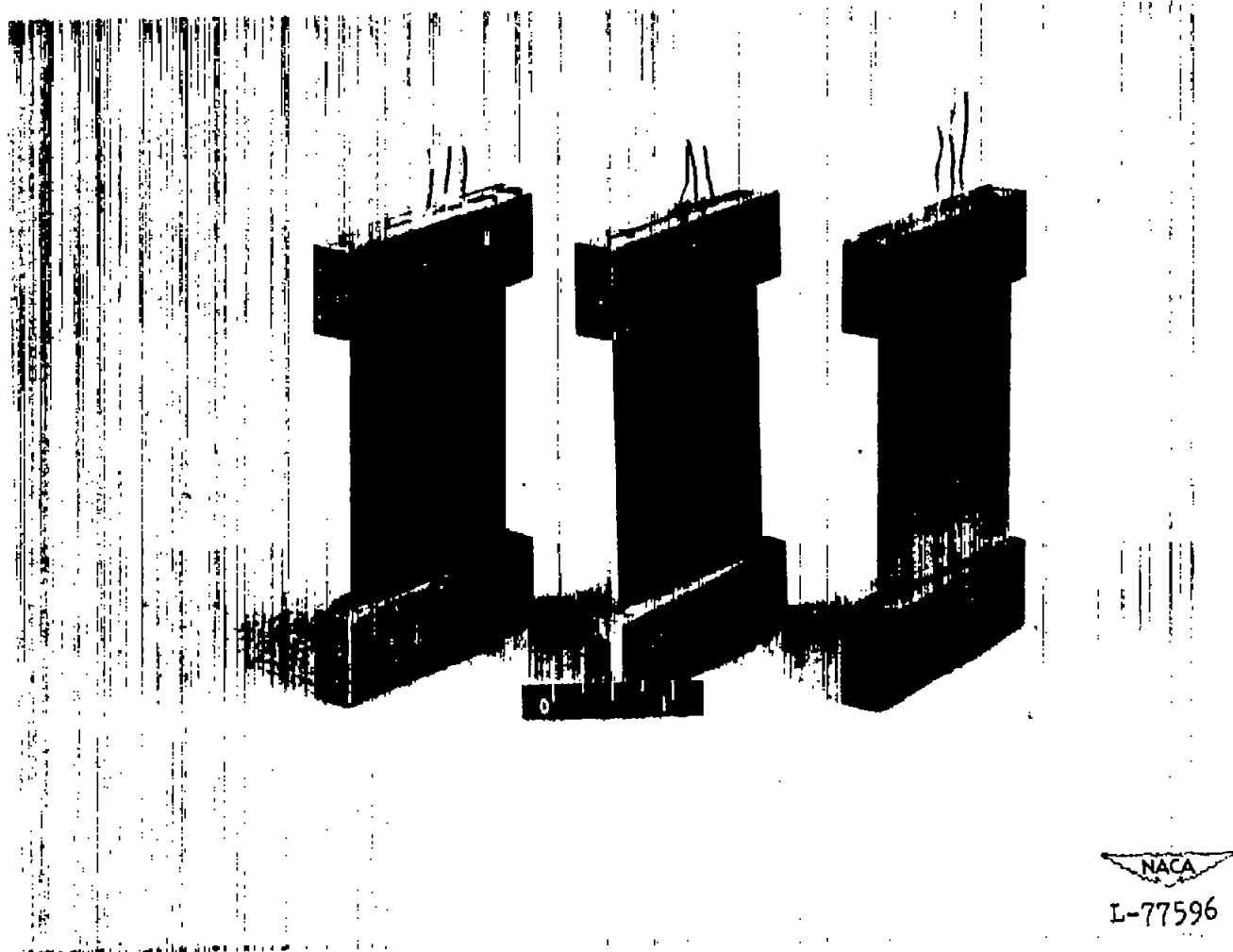
(a) General arrangement.

Figure 1.- Test setup and models.



(b) Test-section arrangement.

Figure 1.- Continued.



(c) Models.

Figure 1.- Concluded.

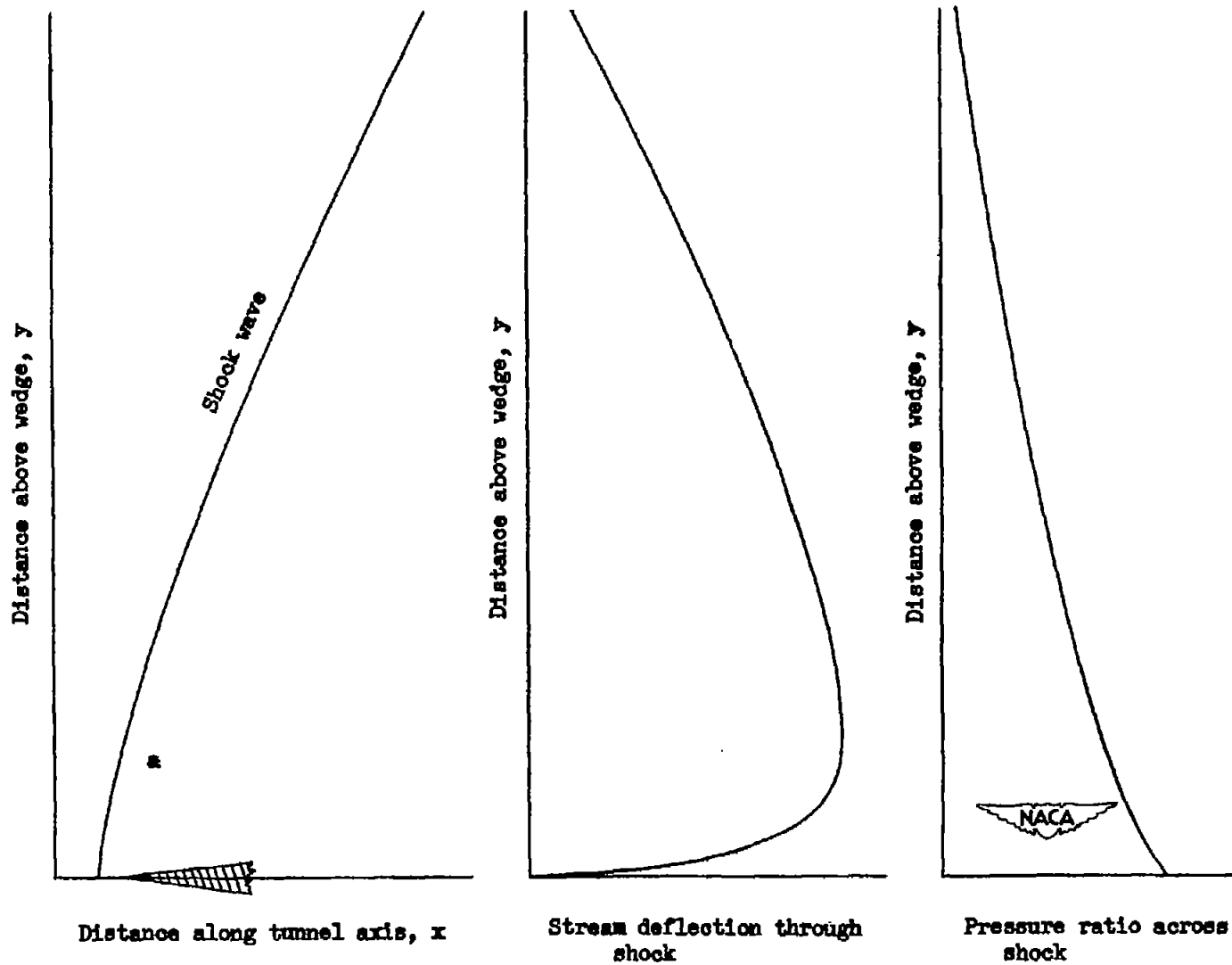
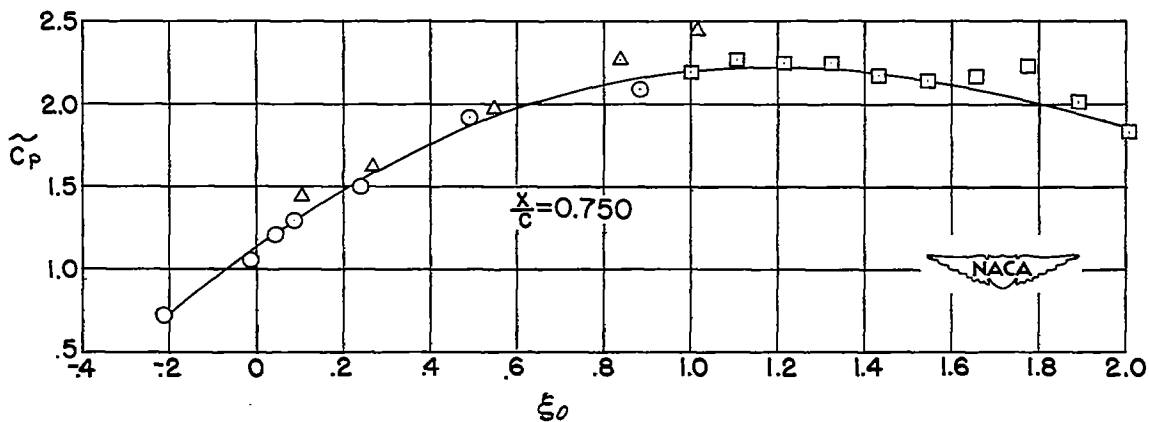
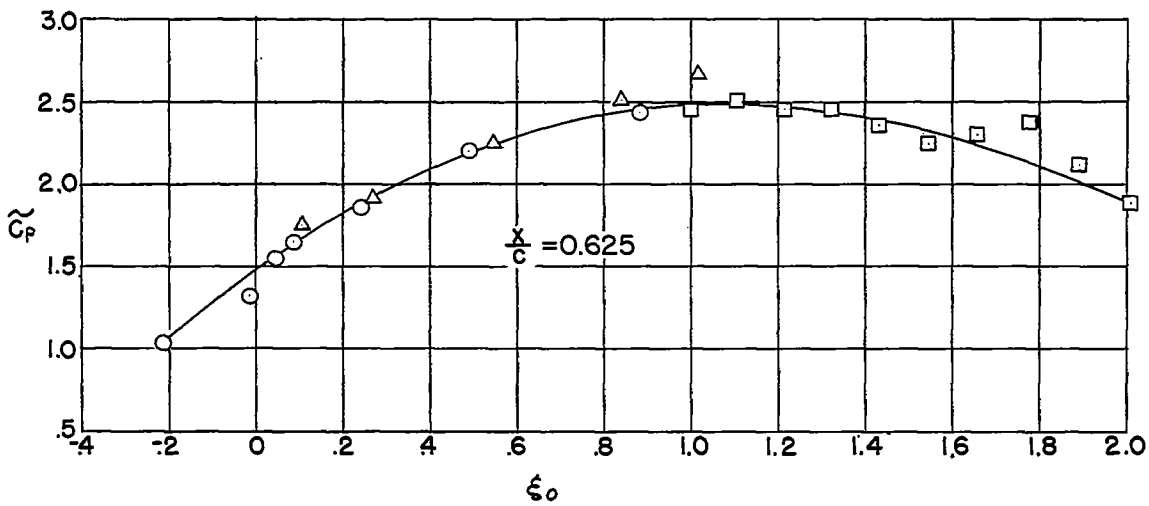
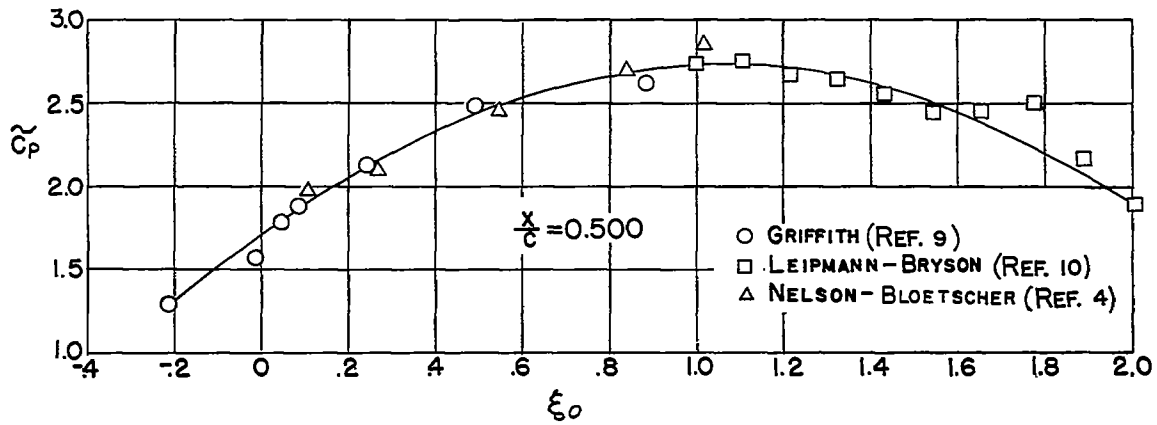
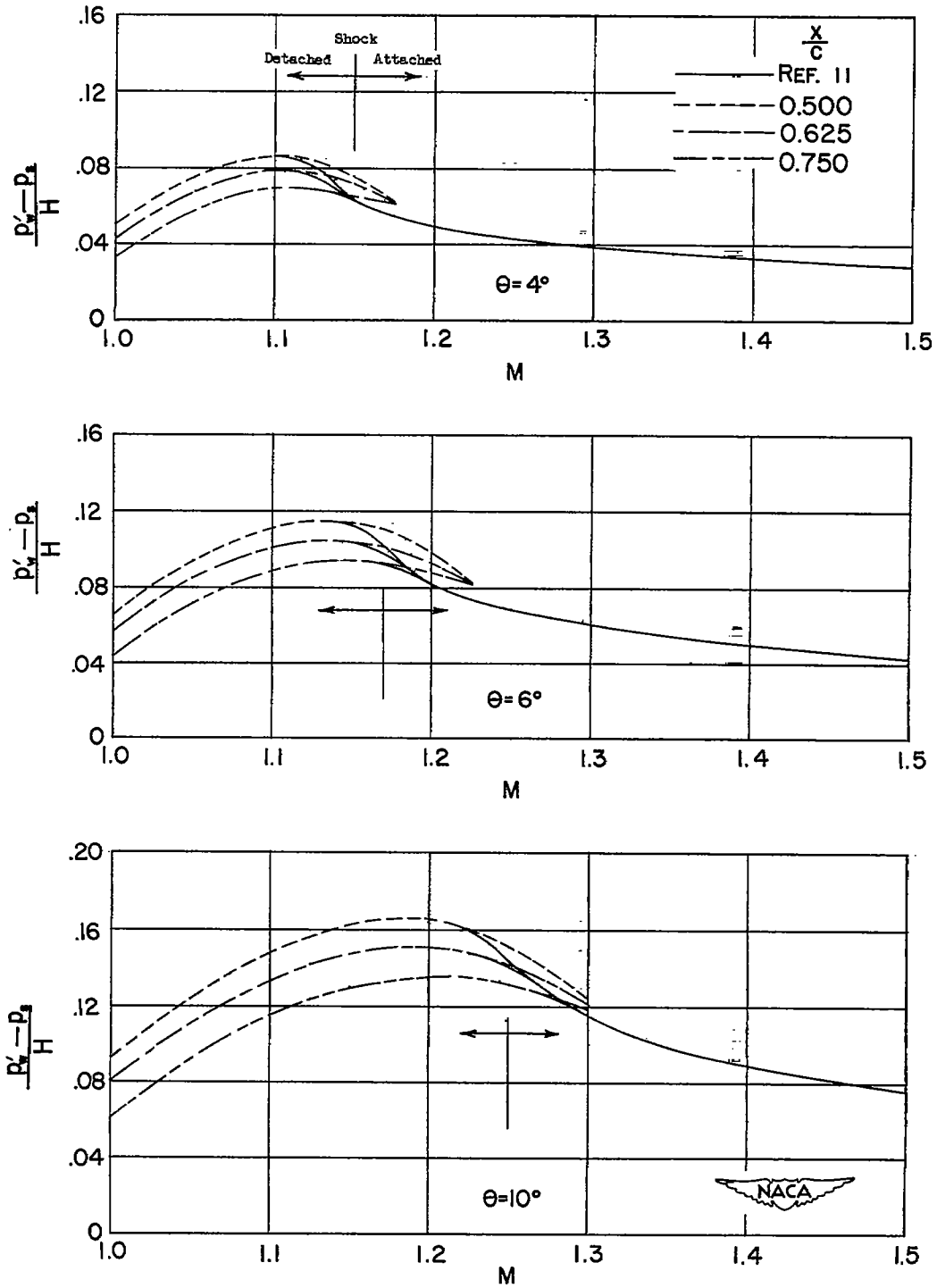


Figure 2.- Detached shock characteristics.



(a) Generalized pressure coefficient against similarity-speed parameter for transonic flow.

Figure 3.- Interference-free pressure distribution over wedges.



(b) Pressure ratio against Mach number for test wedges.

Figure 3.- Concluded.

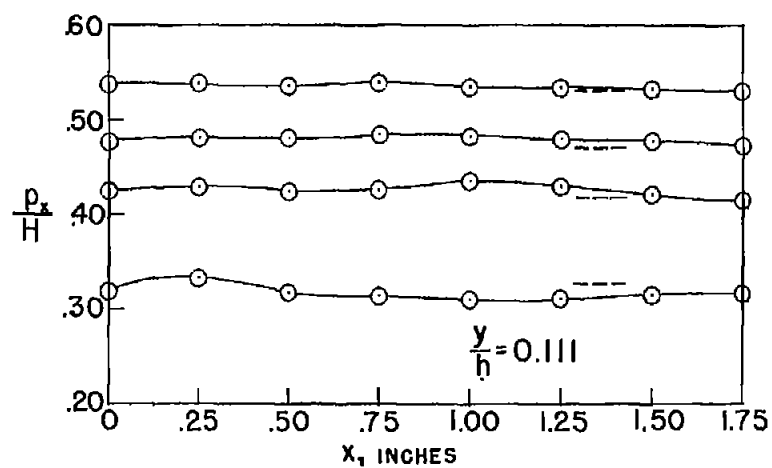
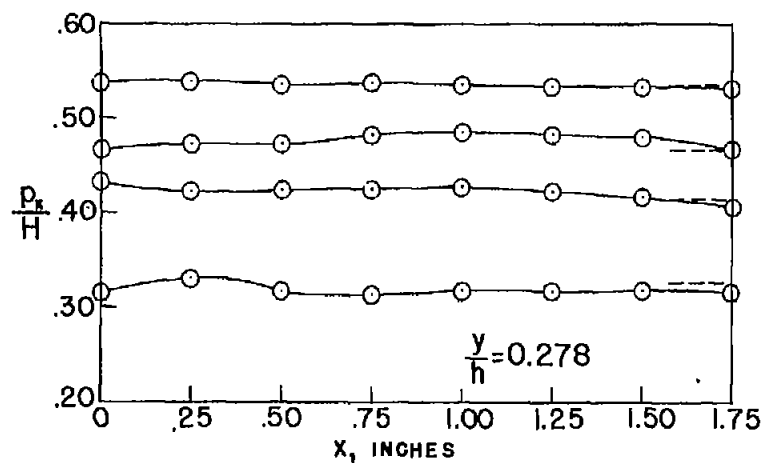
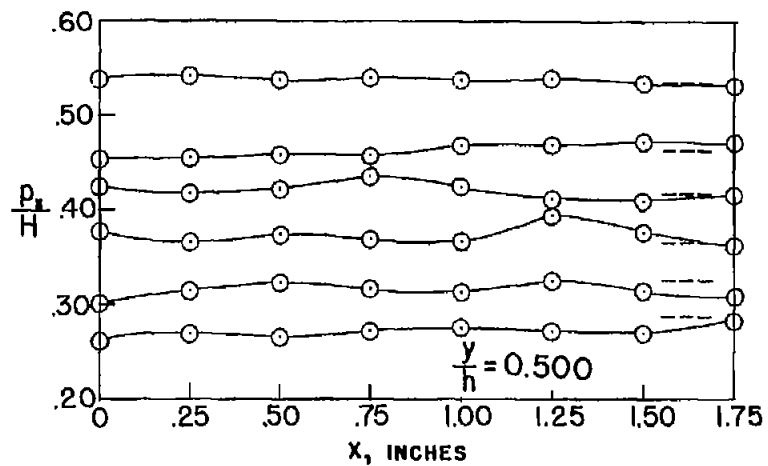
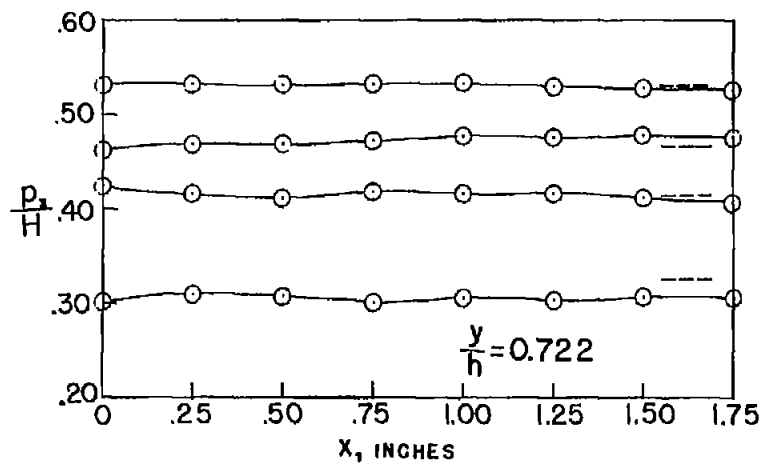
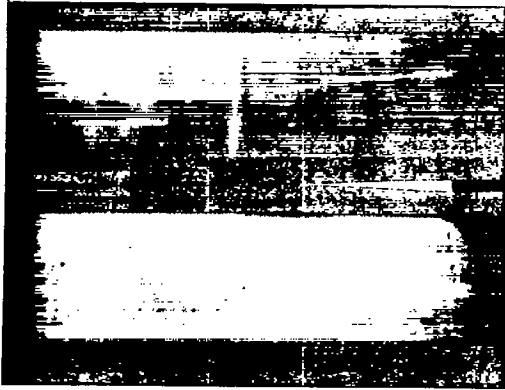
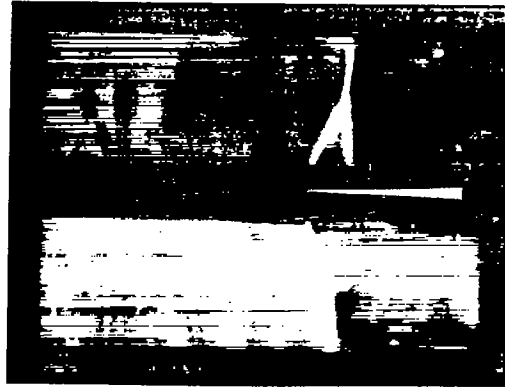


Figure 4.- Pressure distribution in test section with model removed.



M=1.04



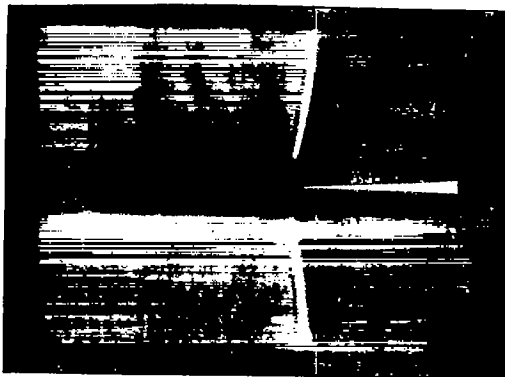
M=1.15



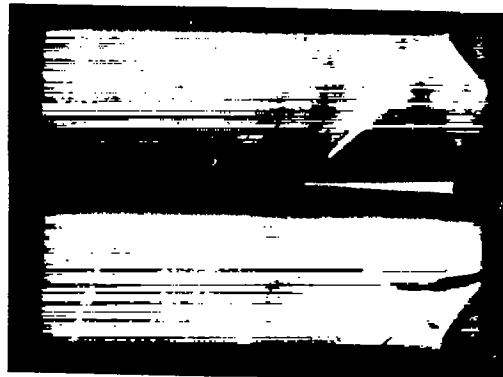
M=1.07



M=1.19



M=1.13



M=1.36

(a) Wedge apex angle, 4° .

L-80201

Figure 5.- Schlieren photographs of flow along slotted walls with model in test section.



M=1.10



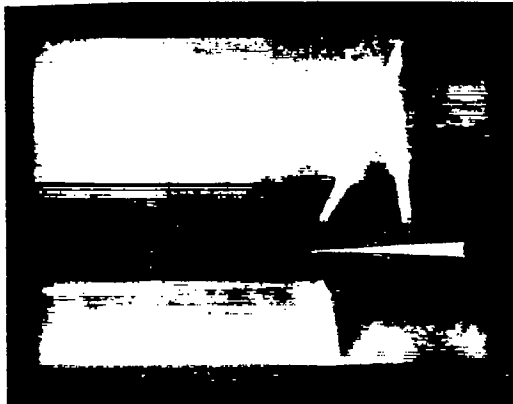
M=1.27



M=1.20



M=1.32



M=1.26



M=1.36

(b) Wedge apex angle, 6° .

Figure 5.- Concluded.

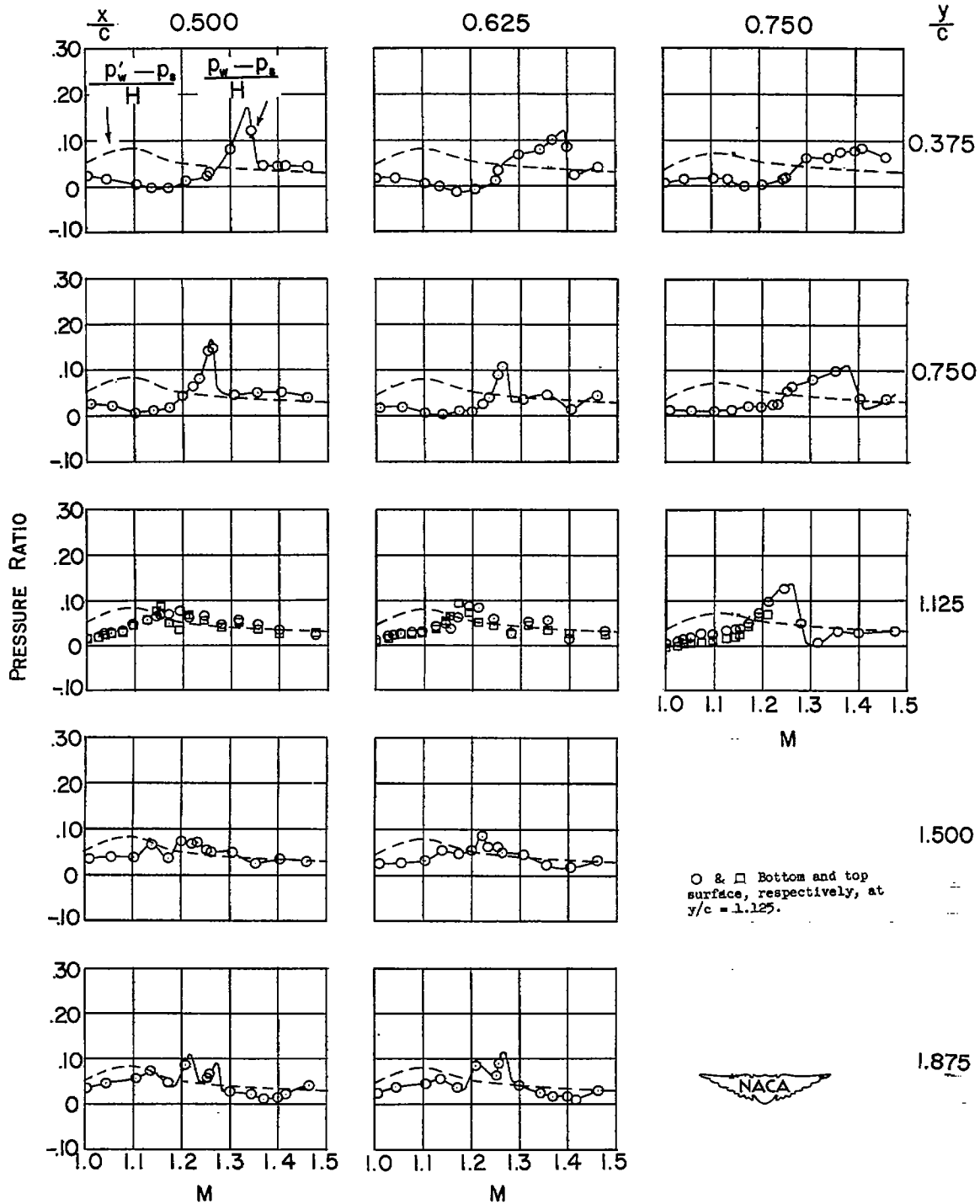
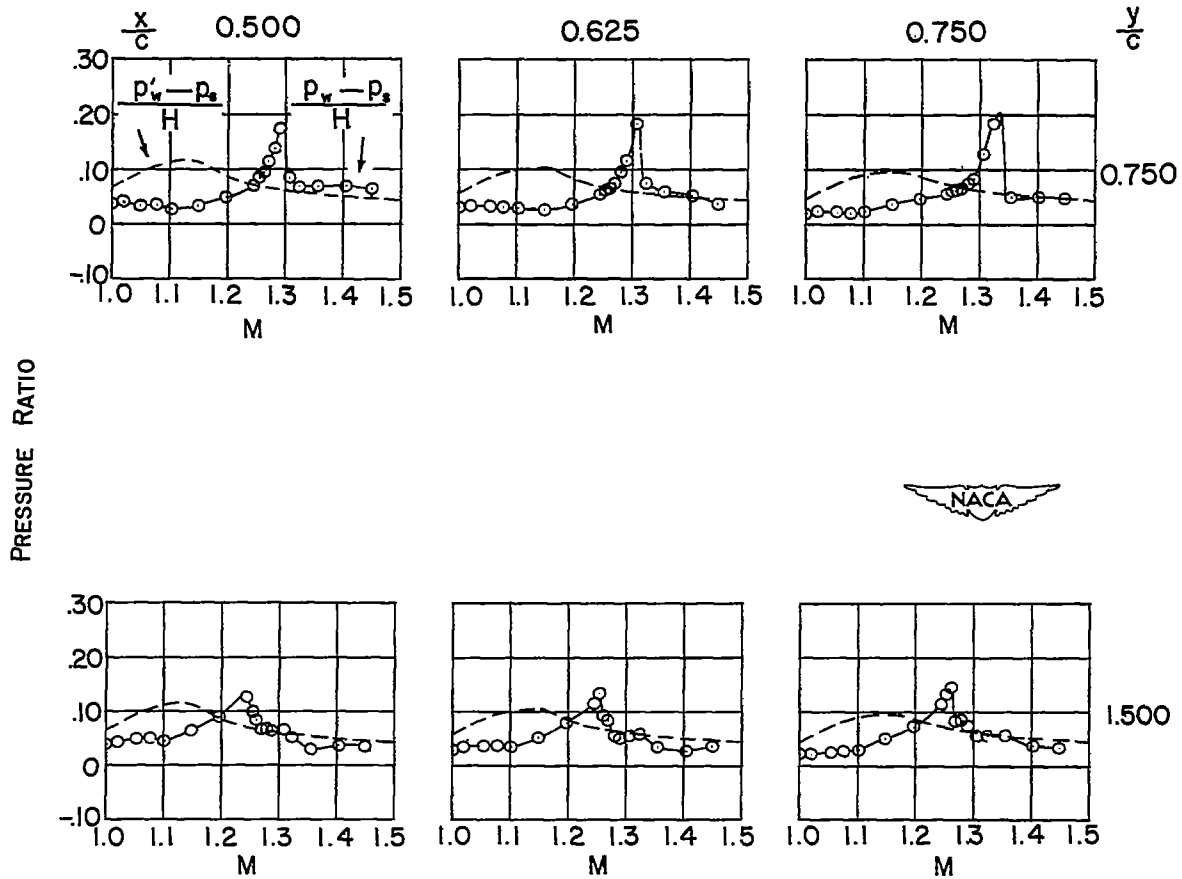
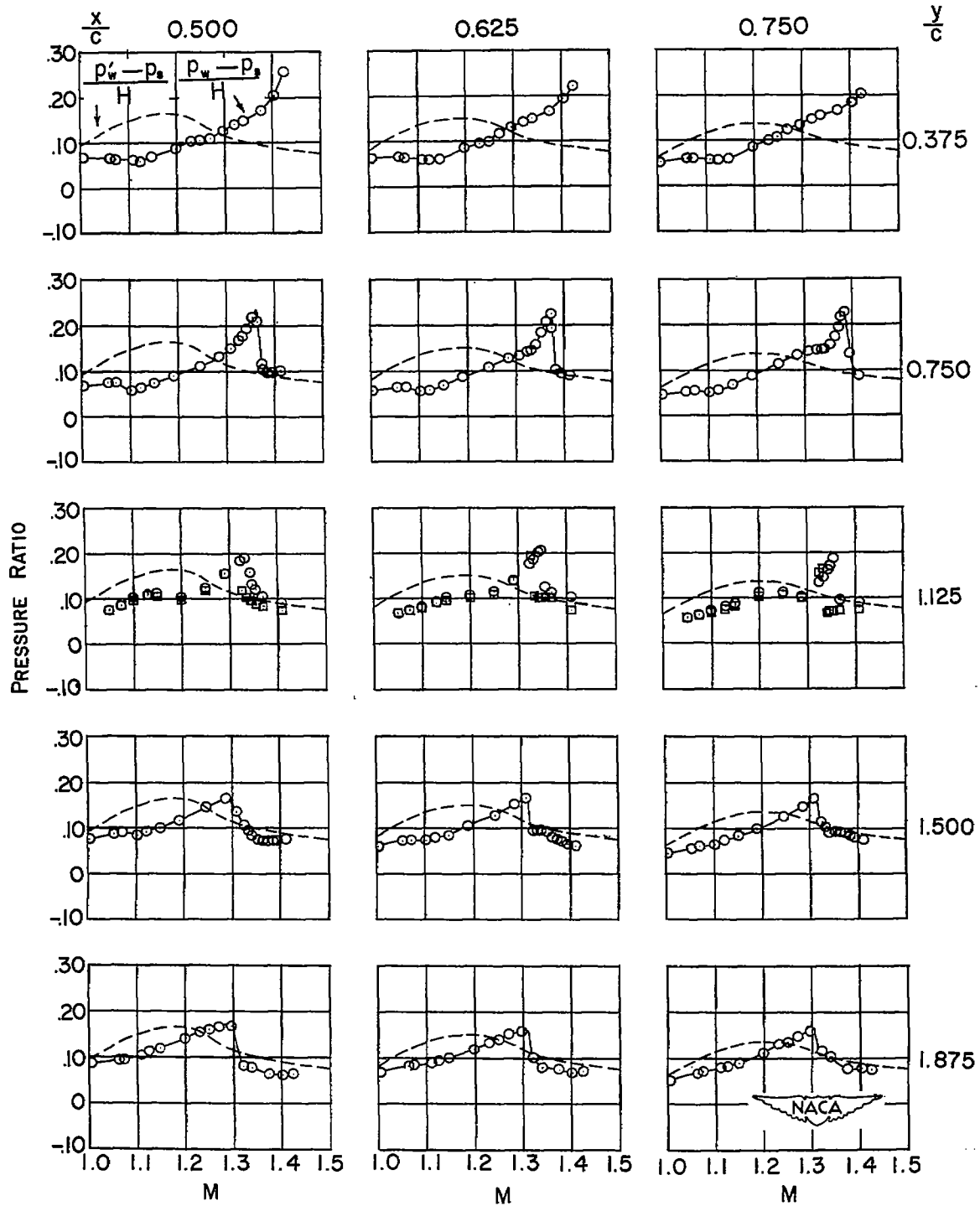
(a) Wedge apex angle, 4° .

Figure 6.- Surface pressure distribution for wedges in slotted jet.



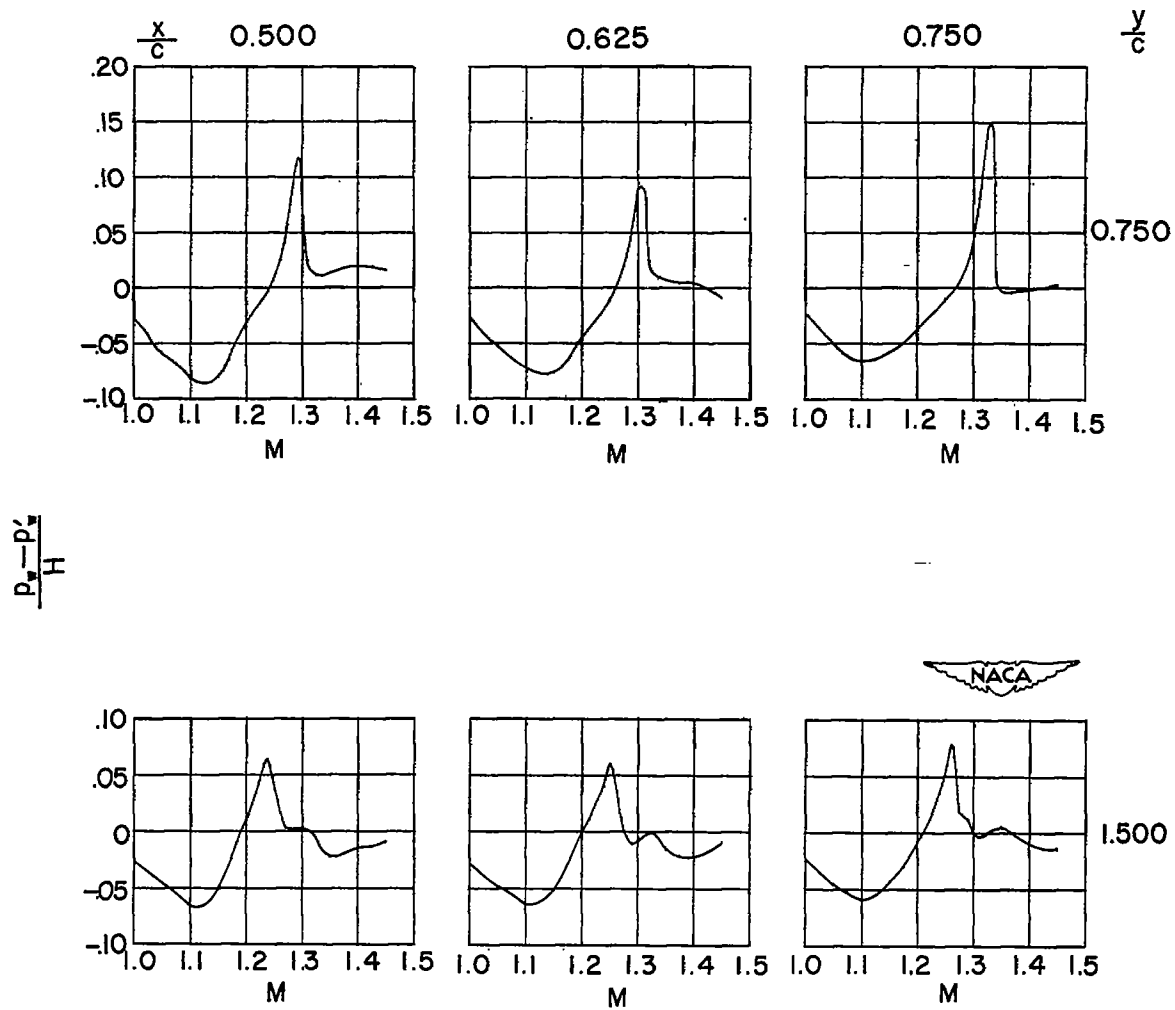
(b) Wedge apex angle, 6°.

Figure 6.- Continued.



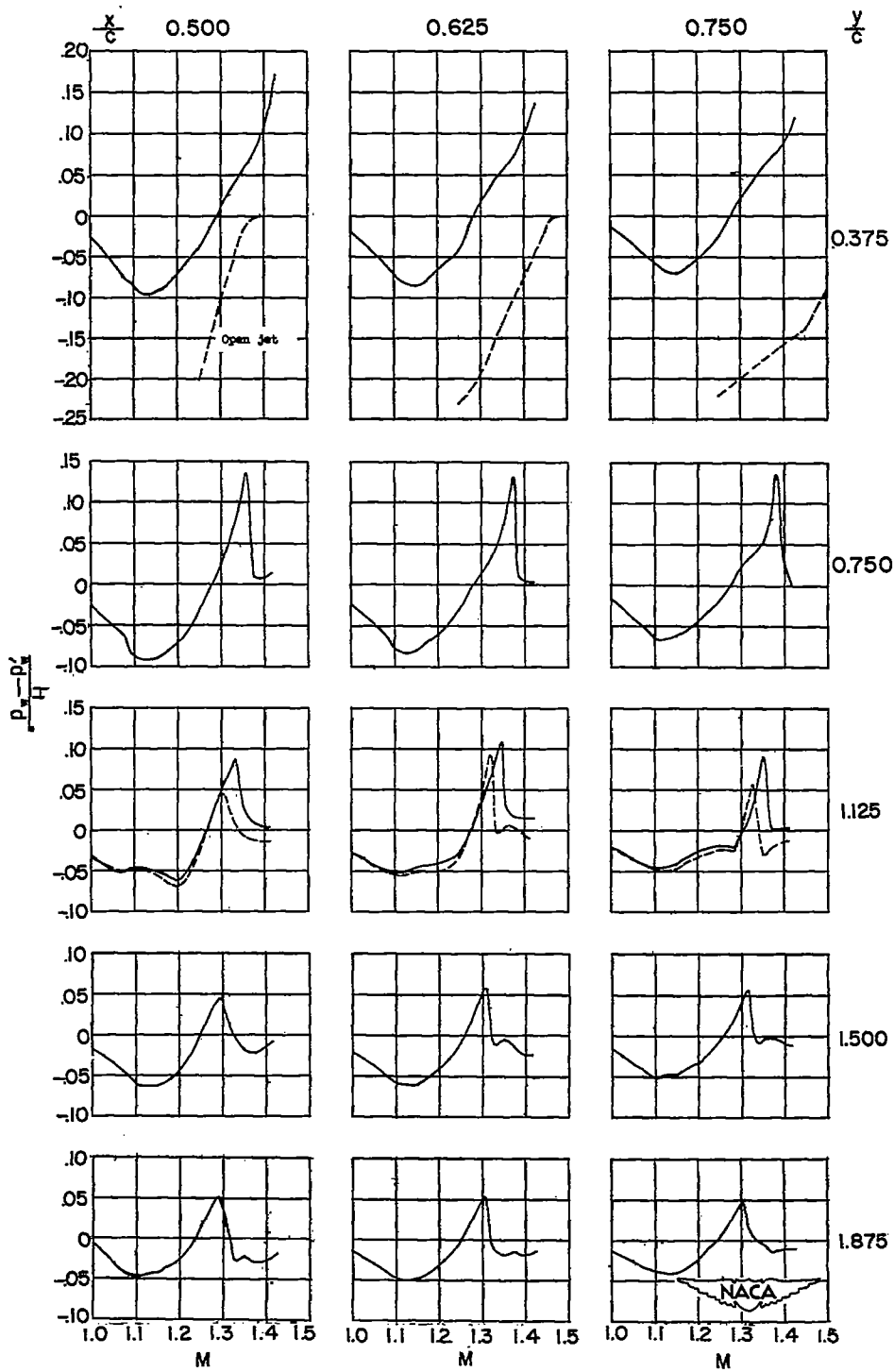
(c) Wedge apex angle, 10° .

Figure 6.- Concluded.



(b) Wedge apex angle, 6° .

Figure 7.- Continued.



(c) Wedge apex angle, 10° .

Figure 7.- Concluded.